JOURNAL OF THEORETICAL AND APPLIED MECHANICS
49, 3, pp. 705-725, Warsaw 2011

EXACT SOLUTIONS FOR FREE VIBRATIONS OF A STEEL-CONCRETE BRIDGE

Luca Della Longa
Antonino Morassi
Anna Rotaris

University of Udine, Department of Civil Engineering and Architecture, Udine, Italy
e-mail: antonino.morassi@uniud.it

This paper deals with a class of free vibrations for a two-span, two-lane steel-concrete bridge. The deck structure is modeled as a thin, homogeneous, orthotropic plate stiffened by beams running along the longitudinal direction of the bridge. The method of separation of variables is used to find exact solutions for a class of free vibrations of the structure. A comparison between analytical and experimental natural frequencies and vibration modes of the bridge is presented and discussed.

Key words: vibrations, bridges, orthotropic plate, eigenvalue problem, exact solutions

1. Introduction

The derivation of accurate mechanical models is one of the main challenges in modern analysis of structural dynamics. The development of such models is of great interest in the study of bridge structures, especially for structural control, damage detection and health monitoring purposes, see (Aktan *et al.*, 1997; Gentile and Cabrera, 1997; Gentile, 2006; Morassi and Vestroni, 2008; Dilena and Morassi, 2011). In the context of structural identification based on dynamic testing, for example, analytical modelling plays a crucial role both in the interpretation of measurements and in the application of Model Updating procedures. Moreover, it has been recognized in the Structural Identification applications that one can hardly obtain anything good without a relatively simple class of physical models which, however, must be able to describe within a certain degree of accuracy the behavior of the real system, see, for example, the papers (Jaishi and Ren, 2005; Gorman and Garibaldi, 2006; Catbas *et al.*, 2007; Morassi and Tonon, 2008a,b; Marcuzzi and Morassi, 2010).

This paper deals with the dynamic behavior of the two-span, two-lane steel-concrete bridge shown in Fig. 1. The bridge belongs to the new highway connecting the cities of Pordenone and Conegliano, in the Friuli Venezia Giulia, a region located in the North East of Italy. Steel-concrete composite structures are largely employed in bridge engineering, especially for bridge decks where a severe control of deformability is needed under important weights during operation. The bridge under study belongs to the rather common class of steel-concrete bridges in which the reinforced concrete slab deck is stiffened transversally by means of steel beams, and these beams, in their turn, are connected at the ends to longitudinal steel plate girders of large cross-section.

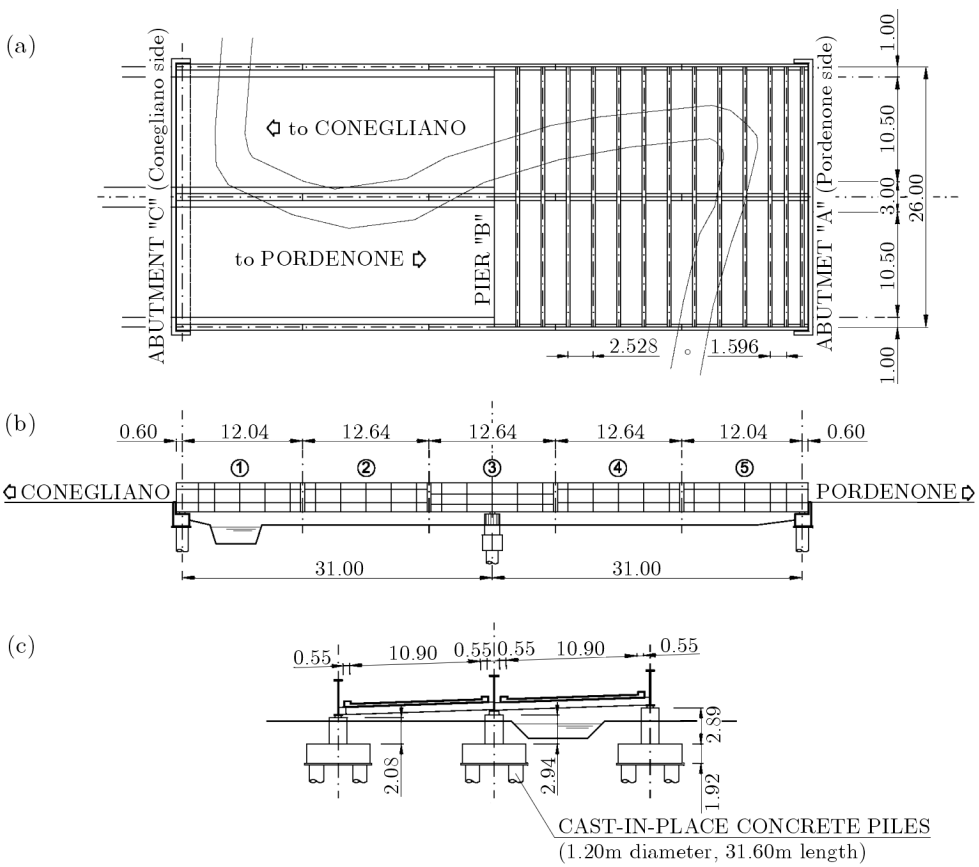

Fig. 1. Zigana bridge: (a) plan, (b) side view and (c) transversal cross-section (lengths in meters)

The object of the present study is twofold. First, to develop a simplified analytical model able to accurately describe the dynamic behavior of this class of steel-concrete bridges. Secondly, to derive an exact solution for a class of free vibrations of the bridge, namely for vibrating modes which are antisymmetric about the transversal symmetry axis of the bridge (e.g., the x_2-axis in Fig. 3).

In the modeling process, the bridge deck is described as two identical homogeneous, orthotropic rectangular plates. Each plate is assumed to be connected by means of cylindrical hinges along the external edge to a reinforcing beam and is simply supported along the two orthogonal edges. Moreover, the two deck plates are connected together by means of cylindrical hinges to the central reinforcing beam running along the common edge, which coincides with the longitudinal bridge axis.

Concerning the plate eigenvalue problem, there is a vast literature on exact solutions for rectangular plates, see, for example, the paper Leissa (1973) for a comprehensive treatment of the isotropic case and Li (2000) for exact solutions for multi-step orthotropic shear plates. The determination of exact solutions for the free vibration of rectangular plates reinforced with beams running along their boundary has undergone growing interest in the recent years. The paper by Cox and Benfield (1959) seems to be the first contribution on this subject. In (Cox and Benfield, 1959), the finite difference method was used to estimate the first frequencies of a uniform isotropic square plate having pinpoint supports at the four corners and flexible beams along the edges. Elishakoff and Sternberg (1980) investigated the vibration of a thin, homogeneous, isotropic, rectangular plate stiffened along two parallel edges and simply supported along the other two. In their study, the torsional vibration of the beam stiffeners was also considered. Gorman (2003) presented a comprehensive study of analytical type solutions for the free vibration of a thin, homogeneous, isotropic corner-supported rectangular plate with symmetrically distributed reinforcing beams attached to the plate edges. The beam reinforcement was treated in the most general case in (Gorman, 2003) by taking into account both bending and rotational stiffness of the beams as well their lateral and rotational inertia.

All these results are valid for a single rectangular plate. In the present case, the study of the free vibration of the bridge leads to an eigenvalue problem for a system formed by *two* uniform, orthotropic rectangular plates. The method of separation of variables is used to find the exact eigenpairs of the system. A comparison between the analytical and experimental natural frequencies of the bridge is also presented and discussed.

2. Description of the bridge

Zigana bridge is a two-span, two-lane steel-concrete composite structure shown in Fig. 1. The bridge deck is formed by a reinforced concrete (r.c.) slab, of thickness 0.25 m, supported by transverse double-T steel beams of height 0.63 m. The deck has a composite structure and the r.c. slab is connected to transverse steel beams by means of steel connectors welded on the upper flange of the beams. The end section of each transverse beam is connected by a bolted joint to the longitudinal main beams, see Fig. 2b. In fact, the whole bridge deck is supported by three continuous, two-span double-T girders of height 2.85 m. The cross-section of each girder was obtained by welding the web panel with the upper and lower flange, and additional flange splices have been inserted to stiffer the beams on the region around the inner support, see Fig. 2a. Finally, five beam elements, each 12.64 m long, were assembled by means of bolted joints to obtain longitudinal continuous beams resting on three supports. Each

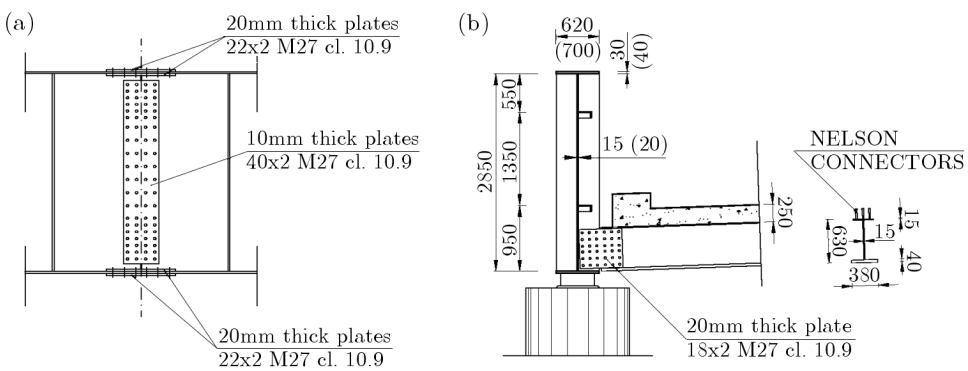

Fig. 2. Constructional details of Zigana bridge: (a) bolted joint of the longitudinal plate girders and (b) bolted connection between longitudinal plate girders and transverse beams. In figure (b), the measures in parentheses are referred to the central plate girder (lengths in millimeters)

longitudinal beam is supported on steel Polytetrafluoroethylene bearing devices at the ends and at the middle point. The inner support of the central girder does not allow any longitudinal or transversal displacement, while at the end supports the transversal (horizontal) movement is constrained. The longitudinal displacement of the two lateral longitudinal beams is restrained at the inner support, while the in-plane motions are free at the end supports. The inner support is on a pile foundation with two or four cast-in-place r.c. piles of 1.2 m diameter and 31.6 m length, for the lateral and the central girder respectively. The abutments consist of an horizontal r.c. beam of solid square

cross-section of side 1.3 m, mounted on a single pile at both ends and on two piles on the middle.

Construction of the bridge was completed in the Fall 2004. It was designed under the Italian Standard Specifications for Highway Bridges in Seismic Areas (D.M. 4/5/1990, Circ. Min. LL.PP. 34233, 25/2/1991, and others). Dynamic and static tests on the bridge were carried out in December 2004 and June 2006, respectively.

With reference to Fig. 3, our mechanical modelling of Zigana bridge is based on the following assumptions:

i) The bridge deck is described as a plate reinforced by a set of equidistant ribs along the x_2-direction (orthotropic plate).

ii) The connections between the deck and the main longitudinal beams are modeled as ideal continuous cylindrical hinges allowing rotation around the x_1-direction. The hinges are assumed to be located on the vertical plane containing the shear center line of the main plate girders.

iii) The bridge deck is assumed to be simply supported at the external edges (parallel to the x_2-direction) and at the central line support (x_2-axis).

Under the above hypotheses and assuming uniform mechanical properties, the analytical model of the bridge is symmetric about the x_2-axis and, therefore, the vibrating modes of the vertical free vibrations split into two sets of symmetric and antisymmetric modes about the x_2-axis. The analysis developed in this paper will concern with an exact solution for the class of x_2-antisymmetric free vibrations of the bridge.

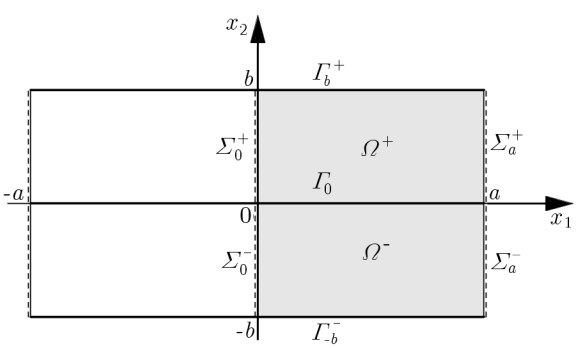

Fig. 3. Schematic view of the bridge deck. Thick line: longitudinal beams; dashed line: supports

3. Formulation of the free vibration problem

Consider the bridge deck structure of Fig. 3 formed by two rectangular plates

$$\begin{aligned} \Omega^+ &= \{(x_1, x_2) \mid \quad 0 < x_1 < a, \;\; 0 < x_2 < b\} \\ \Omega^- &= \{(x_1, x_2) \mid \quad 0 < x_1 < a, \quad -b < x_2 < 0\} \end{aligned} \tag{3.1}$$

connected with three beams parallel to the x_1-direction. The opposite edges of the plates Ω^+, Ω^- parallel to the x_2-direction, namely

$$\begin{aligned} \Sigma_0^+ &= \{(x_1, x_2) \mid \quad x_1 = 0, \;\; 0 < x_2 < b\} \\ \Sigma_a^+ &= \{(x_1, x_2) \mid \quad x_1 = a, \;\; 0 < x_2 < b\} \qquad \text{for } \Omega^+ \end{aligned} \tag{3.2}$$

and

$$\begin{aligned} \Sigma_0^- &= \{(x_1, x_2) \mid \quad x_1 = 0, \quad -b < x_2 < 0\} \\ \Sigma_a^- &= \{(x_1, x_2) \mid \quad x_1 = a, \quad -b < x_2 < 0\} \qquad \text{for } \Omega^- \end{aligned} \tag{3.3}$$

are assumed to be simply supported. The lateral edges along the x_1-direction

$$\begin{aligned} \Gamma_b^+ &= \{(x_1, x_2) \mid \quad 0 < x_1 < a, \;\; x_2 = b\} \\ \Gamma_{-b}^- &= \{(x_1, x_2) \mid \quad 0 < x_1 < a, \;\; x_2 = -b\} \end{aligned} \tag{3.4}$$

of Ω^+ and Ω^-, respectively, are connected by cylindrical hinges to two simply-supported beams. These hinges allow rotation around the x_1-direction. Moreover, the two plates Ω^+ and Ω^- are connected together along the line

$$\Gamma_0 = \{(x_1, x_2) \mid \quad 0 < x_1 < a, \;\; x_2 = 0\} \tag{3.5}$$

to the central beam by means of cylindrical hinges allowing rotation around the x_1-direction. The central beam is simply supported at the ends.

The present analysis is restricted to the case when the system undergoes infinitesimal transversal motion (e.g., in the direction orthogonal to the plane (x_1, x_2)). The beams are described within the Euler-Bernoulli bending theory, whereas an orthotropic Kirchhoff-Love model is used to describe the behavior of the plate deck, see, for example, (Timoshenko, 1959). Accordingly, the spatial description of the undamped vibrations is governed by the Rayleigh quotient of the system

$$R: \; \mathfrak{D} \to \mathbb{R} \tag{3.6}$$

where $\mathfrak{D}$ is the space of the admissible kinematic configurations. The space $\mathfrak{D}$ is defined as the set of functions

$$(w, v^+, v_0, v^-) \in (H^2(\Omega^+) \cup H^2(\Omega^-)) \times H^2(0,a) \times H^2(0,a) \times H^2(0,a) \quad (3.7)$$

such that

$$\begin{aligned} & w = \begin{cases} v^+ & \text{on} \quad \Gamma_b^+ \\ v^- & \text{on} \quad \Gamma_{-b}^- \end{cases} \\ & w(x_1, 0^+) = v_0(x_1) = w(x_1, 0^-) \qquad \text{on} \quad \Gamma_0 \\ & w = 0 \qquad \text{on} \quad \Sigma_0^+ \cup \Sigma_0^- \quad \text{and on} \quad \Sigma_a^+ \cup \Sigma_a^- \\ & v^+(0) = 0 = v^+(a) \qquad\qquad v_0(0) = 0 = v_0(a) \\ & v^-(0) = 0 = v^-(a) \end{aligned} \quad (3.8)$$

Here, $H^m(A)$, with $m \geqslant 1$ integer number and A bounded domain in $\mathbb{R}^n$, $n \geqslant 1$, denotes the standard Sobolev space formed by the measurable functions f such that both f and its derivatives (in the sense of distributions) up to the mth order are square summable functions in A, see (Brezis, 1986). In Eqs. (3.7) and (3.8), $w = w(x_1, x_2)$ is the transversal displacement of the plate and $v^+ = v^+(x_1)$, $v_0 = v_0(x_1)$, $v^- = v^-(x_1)$ is the transversal deflection of the beam lying on the interval Γ_b^+, Γ_0, Γ_{-b}^-, respectively.

On the above assumption, the Rayleigh quotient of the vibrating system has the following expression

$$R[w, v^+, v_0, v^-] = \frac{E}{T} \quad (3.9)$$

where the *elastic energy* E and the *kinetic energy* T are given respectively by

$$\begin{aligned} E[w, v^+, v_0, v^-] = & - \int\limits_{\Omega^+ \cup \Omega^-} M_{\alpha\beta}(w) w_{,\alpha\beta} \; dx_1 dx_2 + \int\limits_{\Gamma_b^+} J(w''(x_1, b))^2 \; dx_1 \\ & + \int\limits_{\Gamma_0} J_0(w''(x_1, 0))^2 \, d dx_1 + \int\limits_{\Gamma_{-b}^-} J(w''(x_1, -b))^2 \; dx_1 \\ T[w, v^+, v_0, v^-] = & \int\limits_{\Omega^+ \cup \Omega^-} \rho_p w^2 \; dx_1 dx_2 + \int\limits_{\Gamma_b^+} \rho_b w^2(x_1, b) \; dx_1 \\ & + \int\limits_{\Gamma_0} \rho_{b0} w^2(x_1, 0) \; dx_1 + \int\limits_{\Gamma_{-b}^-} \rho_b w^2(x_1, -b) \; dx1 \end{aligned} \quad (3.10)$$

In the above expressions, $M_{11}(w)$, $M_{22}(w)$ are the bending moments and $M_{12}(w) = M_{21}(w)$ are the torsional moments of the plate associated to the transversal deflection w. The following constitutive equations can be assumed for $M_{\alpha\beta}$

$$\begin{aligned} M_{11}(w) &= -(D_{11}w_{,11} + D_1 w_{,22}) \\ M_{22}(w) &= -(D_{22}w_{,22} + D_1 w_{,11}) \\ M_{12}(w) &= -2D_{12}w_{,12} \end{aligned} \tag{3.11}$$

where the constants $D_{11} > 0$, $D_{22} > 0$, $D_{12} > 0$ are the two flexural and the torsional rigidity of the orthotropic plate, respectively, and $D_1 > 0$ is the term which takes into account the transverse contraction of the plate, see (Timoshenko, 1959). In Eq. (3.10), J and J_0 are the uniform bending stiffness of the two lateral longitudinal beams and of the central beam, respectively. Further, ρ_p, ρ_b, ρ_{b0} are the surface mass density of the plate, the linear mass density of the two lateral beams and of the central beam, respectively.

The differential formulation of the free vibration problem for the system is obtained by imposing the stationarity of Rayleigh quotient (3.9) on the set $\mathfrak{D}$ defined by Eqs. (3.7) and (3.8), see (Weinberger, 1965). The eigenvalue problem consists in determining the eigenpair $\{\omega^2 > 0;\ w \in H^4(\Omega^+) \cup H^4(\Omega^-)\}$, with $w(x_1, \pm b) \in H^4(0, a)$ and $w(x_1, 0) \in H^4(0, a)$, such that

$$\begin{aligned} & D_{11}w_{,1111} + 2Hw_{,1122} + D_{22}w_{,2222} = \omega^2 \rho_p w \qquad \text{in } \Omega^+ \cup \Omega^- \\ & w_{,22} = 0 \qquad \text{on } \Gamma_b^+ \cup \Gamma_{-b}^- \cup \Gamma_0 \\ & [\![w]\!] = 0 \qquad \text{on } \Gamma_0 \\ & \widetilde{H}w_{,112} + D_{22}w_{,222} = \begin{cases} Jw_{,1111} - \omega^2 \rho_b w & \text{on } \Gamma_b^+ \\ -(Jw_{,1111} - \omega^2 \rho_b w) & \text{on } \Gamma_{-b}^- \end{cases} \\ & \widetilde{H}[\![w_{,112}]\!] + D_{22}[\![w_{,222}]\!] = -(J_0 w_{,1111} - \omega^2 \rho_{b0} w) \qquad \text{on } \Gamma_0 \\ & w = 0 \qquad \text{on } \overline{\Sigma}_0^+ \cup \overline{\Sigma}_0^- \cup \overline{\Sigma}_a^+ \cup \overline{\Sigma}_a^- \\ & w_{,11} = 0 \qquad \text{on } \overline{\Sigma}_0^+ \cup \overline{\Sigma}_0^- \cup \overline{\Sigma}_a^+ \cup \overline{\Sigma}_a^- \end{aligned} \tag{3.12}$$

where $H = 2D_{12} + D_1$, $\widetilde{H} = 4D_{12} + D_1$, $[\![w]\!] \equiv w(x_1, 0^+) - w(x_1, 0^-)$, $[\![w_{,112}]\!] \equiv w_{,112}(x_1, 0^+) - w_{,112}(x_1, 0^-)$. Here, $\overline{\Sigma}_0^+ = [0, b]$. From the mechanical point of view, boundary condition $(3.12)_2$ expresses the vanishing of bending moment and conditions $(3.12)_{4-6}$ express the equilibrium of the forces acting in the direction transversal to the plane (x_1, x_2) along the lines Γ_b^+, Γ_{-b}^-, Γ_0, respectively.

The differential operator governing eigenvalue problem (3.12) is a self-adjoint compact operator in $\mathfrak{D}$ and, therefore, by general results (see Brezis,

1986) (i) there exists a countable number of real eigenvalues ω_n^2, $n = 1, 2, \ldots$, with $\omega_n^2 > 0$, and such that $\lim_{n\to\infty} \omega_n^2 = \infty$; (ii) eigenfunctions associated to distinct eigenvalues are orthogonal with respect to the mass distribution; (iii) there exists a countable base of the space $\mathfrak{D}$ formed by the eigenfunctions of the problem. It is worth noticing that if $w(x_1, x_2)$ is an eigenfunction of boundary value problem (3.12), then it can be extended as

$$w(-x_1, x_2) = -w(x_1, x_2) \qquad (x_1, x_2) \in \overline{\Omega}^+ \cup \overline{\Omega}^- \tag{3.13}$$

to obtain the corresponding x_2-antisymmetric mode shape of the whole bridge structure in the rectangle $[-a, a] \times [-b, b]$, see Fig. 3.

4. Exact free vibration solutions

The exact solutions to eigenvalue problem (3.12) will be determined by means of a variant of the method of separation of variables, see, e.g., (Voigt, 1893). It is assumed that a non-trivial solution to boundary-value problem (3.12) can be found in the form

$$w(x_1, x_2) = X(x_1)Y(x_2) \tag{4.1}$$

By substituting Eq. (4.1) into Eq. $(3.12)_1$ and dividing by w, it follows that

$$D_{11}\frac{X^{IV}}{X} + 2H\frac{X^{II}}{X}\frac{Y^{II}}{Y} + D_{22}\frac{Y^{IV}}{Y} = \omega^2\rho_p \tag{4.2}$$

where φ^I denotes the first derivative of the function φ with respect to its argument. Taking the partial derivative of Eq. (4.2) with respect to x_2, it follows that

$$2H\frac{X^{II}}{X}\Big(\frac{Y^{II}}{Y}\Big)^I + D_{22}\Big(\frac{Y^{IV}}{Y}\Big)^I = 0 \tag{4.3}$$

which can be separated, yielding

$$X^{II} + \beta X = 0 \qquad \text{in} \quad (0, a) \tag{4.4}$$

where β is the separation parameter. The non trivial solutions to differential equation (4.4) subject to boundary conditions $(3.12)_7$, e.g.

$$X(0) = 0 = X(a) \tag{4.5}$$

are given by

$$X_n(x_1) = \sin\frac{n\pi x_1}{a} \qquad \beta_n = \Big(\frac{n\pi}{a}\Big)^2 \qquad n = 1, 2, \ldots \tag{4.6}$$

It is worth noticing that the eigensolutions $X_n(x_1)$ satisfy also boundary conditions $(3.12)_8$, since $X_n^{II}(0) = X_n^{II}(a) = 0$. Moreover, from Eq. (4.4) one has

$$X_n^{IV} = -\beta_n X_n^{II} = \beta_n^2 X_n \qquad \text{in} \quad (0,a) \tag{4.7}$$

Therefore, by Eq. (4.2), the function $Y \in H^4(-b,0) \cup H^4(0,b)$ must satisfy the ordinary differential equation

$$D_{22}Y^{IV} - 2H\beta_n Y^{II} + (D_{11}\beta_n^2 - \omega^2\rho_p)Y = 0 \qquad \text{in} \quad (-b,0)\cup(0,b) \tag{4.8}$$

the boundary conditions at $x_2 = \pm b$

$$\begin{aligned} &D_{22}Y^{III}(b) - \widetilde{H}\beta_n Y^I(b) = (J\beta_n^2 - \omega^2\rho_b)Y(b) \\ &D_{22}Y^{III}(-b) - \widetilde{H}\beta_n Y^I(-b) = -(J\beta_n^2 - \omega^2\rho_b)Y(-b) \\ &Y^{II}(b) = 0 \qquad\qquad Y^{II}(-b) = 0 \end{aligned} \tag{4.9}$$

and the boundary and jump conditions at $x_2 = 0$

$$\begin{aligned} &Y^{II}(0^+) = 0 \qquad\qquad Y^{II}(0^-) = 0 \\ &[\![Y]\!] = 0 \\ &D_{22}[\![Y^{III}]\!] - \widetilde{H}\beta_n [\![Y^I]\!] = -(J_0\beta_n^2 - \omega^2\rho_{b0})Y(0) \end{aligned} \tag{4.10}$$

where $[\![Y]\!] \equiv Y(0^+) - Y(0^-)$.

Again, by general results, see Brezis (1986), eigenvalue problem (4.8)-(4.10) has a countable number of real, positive eigenvalues for every given n, $n = 1, 2, \ldots$, with the accumulation point at infinity. Therefore, the eigenfunctions of problem (3.12) can be written as

$$w_{n,m}(x_1,x_2) = X_n(x_1)Y_m(x_2) \qquad \begin{matrix} n = 1,2,\ldots \\ m = 1,2,\ldots \end{matrix} \tag{4.11}$$

Looking for solutions of the form $Y(x_2) = \exp(qx_2)$, the characteristic equation for differential equation (4.8) becomes

$$f(z) = z^2 - 4Az + B = 0 \tag{4.12}$$

where

$$z = q^2 \qquad A \equiv \frac{H\beta_n}{2D_{22}} > 0 \qquad B \equiv \frac{D_{11}\beta_n^2 - \omega^2\rho_p}{D_{22}} \tag{4.13}$$

To find the roots of $f(z)$, one has to distinguish the following cases

$$\begin{aligned} &\text{i)} \quad B > 0 \qquad \text{“low” frequency case} \\ &\text{ii)} \quad B < 0 \qquad \text{“high” frequency case} \\ &\text{iii)} \quad B = 0 \qquad \text{“limit” case} \end{aligned} \tag{4.14}$$

Case i). When $B > 0$, the following three subcases have to be considered

$$\begin{aligned} &\text{i1)} \quad 4A^2 - B > 0 \\ &\text{i2)} \quad 4A^2 - B < 0 \\ &\text{i3)} \quad 4A^2 - B = 0 \end{aligned} \tag{4.15}$$

i1) If $4A^2 - B > 0$, then there exist two real positive roots of $f(z)$ such that

$$0 < z_1 < 2A < z_2 \tag{4.16}$$

Therefore

$$\{q_j\}_{j=1}^4 = \{-\sqrt{z_1}, \sqrt{z_1}, -\sqrt{z_2}, \sqrt{z_2}\} \tag{4.17}$$

and the solution to differential equation (4.8), on each interval $(-b, 0)$, $(0, b)$, can be written in the form

$$\begin{aligned} Y(x_2) = C_1 \sinh(\sqrt{z_1}x_2) + C_2 \cosh(\sqrt{z_1}x_2) \\ + C_3 \sinh(\sqrt{z_2}x_2) + C_4 \cosh(\sqrt{z_2}x_2) \end{aligned} \tag{4.18}$$

where C_i, $i = 1, \ldots, 4$, are real constants of integration.

i2) When $4A^2 - B < 0$, the equation $f(z) = 0$ has two complex conjugate roots

$$z_1 = \operatorname{Re} z_1 + \mathrm{i} \operatorname{Im} z_1 \qquad z_2 = \overline{z}_1 \qquad \operatorname{Im} z_1 \neq 0 \tag{4.19}$$

Therefore, putting $q \equiv a + \mathrm{i}b$ such that $q^2 = z_1$, one has

$$\{q_1, q_2, q_3, q_4\} = \{a + \mathrm{i}b, -(a + \mathrm{i}b), a - \mathrm{i}b, -(a - \mathrm{i}b)\} \tag{4.20}$$

The solution of the differential equation (4.8) can be written on each interval as

$$Y(x_2) = \mathrm{e}^{ax_2}[C_1 \cos(bx_2) + C_2 \sin(bx_2)] + \mathrm{e}^{-ax_2}[C_3 \cos(bx_2) + C_4 \sin(bx_2)] \tag{4.21}$$

with four constants of integration C_1, C_2, C_3, C_4.

i3) For $4A^2 = B$, the function $f(z)$ has a double root at $z = 2A$ and the solution of Eq. (4.8) is of the form

$$\begin{aligned} Y(x_2) = C_1 \sinh(\sqrt{2A}x_2) + C_2 x_2 \sinh(\sqrt{2A}x_2) \\ + C_3 \cosh(\sqrt{2A}x_2) + C_4 x_2 \cosh(\sqrt{2A}x_2) \end{aligned} \tag{4.22}$$

with C_i, $i = 1, \ldots, 4$, constants of integration.

Case ii). When $B < 0$, the roots of $f(z) = 0$ are always real and such that $z_1 < 0$ and $z_2 > 2A$. Therefore, putting $q_1 = -\mathrm{i}\sqrt{-z_1}$, $q_2 = \mathrm{i}\sqrt{-z_1}$, $q_3 = -\sqrt{z_2}$, $q_4 = \sqrt{z_2}$, the general solution to Eq. (4.8) is

$$\begin{aligned} Y(x_2) = C_1 \cos(\sqrt{-z_1}x_2) + C_2 \sin(\sqrt{-z_1}x_2) \\ +C_3 \cosh(\sqrt{z_2}x_2) + C_4 \sinh(\sqrt{z_2}x_2) \end{aligned} \tag{4.23}$$

with four constants of integration C_i, $i = 1, \ldots, 4$.

Case iii). Finally, when $B = 0$ there are two real solutions $z_1 = 0$ and $z_2 = 4A$, and the general solution to Eq. (4.8) is of the form

$$Y(x_2) = C_1 + C_2 x_2 + C_3 \cosh(2\sqrt{A}x_2) + C_4 \sinh(2\sqrt{A}x_2) \tag{4.24}$$

with C_i, $i = 1, \ldots, 4$, constants of integration.

By substituting the general solution to equation (4.8) (e.g., the expression (4.18), (4.21), (4.22), (4.23), (4.24) for cases i1), i2), i3), ii), iii), respectively) into the eight boundary and jump conditions (4.9) and (4.10), a homogeneous linear system of eight equations for C_i, C_i', $i = 1, \ldots, 4$, is obtained, e.g. $\mathbf{M}(\omega^2)\boldsymbol{c} = \mathbf{0}$. To find non-trivial solutions for $Y(x_2)$, the determinant $\det \mathbf{M}(\omega^2)$ of the corresponding matrix should be set equal to zero.

The above analysis can be simplified by adopting suitable symmetry considerations. Because of the symmetry of the eigenvalue problem with respect to the x_1-axis, the eigenfunctions of the system (4.8)-(4.10) split into the two sets of x_1-symmetric, $\mathcal{S}$, and x_1-antisymmetric, $\mathcal{A}$, eigenfunctions, namely

$$\begin{aligned} \mathcal{S} &= \{Y(x_2) \ \text{ eigenfunction} \mid \ Y(-x_2) = Y(x_2), \ x_2 \in (-b, b)\} \\ \mathcal{A} &= \{Y(x_2) \ \text{ eigenfunction} \mid \ Y(-x_2) = -Y(x_2), \ x_2 \in (-b, b)\} \end{aligned} \tag{4.25}$$

By way of an example, it will be shown how the analysis simplifies in case i1) ($B > 0, 4A^2 - B > 0$). Symmetric eigenfunctions have the expression

$$Y(x_2) = \begin{cases} C_1 \sinh(\sqrt{z_1}x_2) + C_2 \cosh(\sqrt{z_1}x_2) \\ +C_3 \sinh(\sqrt{z_2}x_2) + C_4 \cosh(\sqrt{z_2}x_2) \quad \text{in} \quad (0, b) \\ -C_1 \sinh(\sqrt{z_1}x_2) + C_2 \cosh(\sqrt{z_1}x_2) \\ -C_3 \sinh(\sqrt{z_2}x_2) + C_4 \cosh(\sqrt{z_2}x_2) \quad \text{in} \quad (-b, 0) \end{cases} \tag{4.26}$$

where the four constants C_1, C_2, C_3, C_4 can be determined by imposing the four linearly independent boundary conditions $(4.9)_{1,3}$ and $(4.10)_{1,3}$. The corresponding 4×4 coefficient matrix $\mathbf{M}_{\mathcal{S}}(\omega^2)$ is

$$\begin{bmatrix} q_1^2 \sinh(q_1 b) & q_1^2 \cosh(q_1 b) & q_2^2 \sinh(q_2 b) & q_2^2 \cosh(q_2 b) \\ m_{21} & m_{22} & m_{23} & m_{24} \\ 0 & q_1^2 & 0 & q_2^2 \\ 2q_1^3 - \widetilde{H}\beta_n q_1 & J_0\beta_n^2 - \omega^2\rho_{b0} & 2q_2^3 - \widetilde{H}\beta_n q_2 & J_0\beta_n^2 - \omega^2\rho_{b0} \end{bmatrix} \tag{4.27}$$

where $q_1 = \sqrt{z_1}$, $q_2 = \sqrt{z_2}$ and

$$\begin{aligned} m_{21} &= (D_{22}q_1^3 - \widetilde{H}\beta_n q_1)\cosh(q_1 b) - (J\beta_n^2 - \omega^2\rho_b)\sinh(q_1 b) \\ m_{22} &= (D_{22}q_1^3 - \widetilde{H}\beta_n q_1)\sinh(q_1 b) - (J\beta_n^2 - \omega^2\rho_b)\cosh(q_1 b) \\ m_{23} &= (D_{22}q_2^3 - \widetilde{H}\beta_n q_2)\cosh(q_2 b) - (J\beta_n^2 - \omega^2\rho_b)\sinh(q_2 b) \\ m_{24} &= (D_{22}q_2^3 - \widetilde{H}\beta_n q_2)\sinh(q_2 b) - (J\beta_n^2 - \omega^2\rho_b)\cosh(q_2 b) \end{aligned} \tag{4.28}$$

Similarly, and always in case i1), the antisymmetric eigenfunctions can be written in the form

$$Y(x_2) = \begin{cases} C_1 \sinh(\sqrt{z_1}x_2) + C_2 \cosh(\sqrt{z_1}x_2) \\ +C_3 \sinh(\sqrt{z_2}x_2) + C_4 \cosh(\sqrt{z_2}x_2) \quad \text{in} \quad (0, b) \\ C_1 \sinh(\sqrt{z_1}x_2) - C_2 \cosh(\sqrt{z_1}x_2) \\ +C_3 \sinh(\sqrt{z_2}x_2) - C_4 \cosh(\sqrt{z_2}x_2) \quad \text{in} \quad (-b, 0) \end{cases} \tag{4.29}$$

and four constants of integration C_i, $i = 1, \ldots, 4$, will be determined from boundary conditions $(4.9)_{1,3}$, $(4.10)_{1,3}$. The corresponding 4×4 coefficient matrix $\mathbf{M}_{\mathcal{A}}(\omega^2)$ is

$$\begin{bmatrix} q_1^2 \sinh(q_1 b) & q_1^2 \cosh(q_1 b) & q_2^2 \sinh(q_2 b) & q_2^2 \cosh(q_2 b) \\ m_{21} & m_{22} & m_{23} & m_{24} \\ 0 & 1 & 0 & 1 \\ 0 & q_1^2 & 0 & q_2^2 \end{bmatrix} \tag{4.30}$$

Remaining cases i2), i3), ii), iii) have been studied analogously.

Finally, in order to determine the natural pulsations as roots of the characteristic equations $\det \mathbf{M}_{\mathcal{S}}(\omega^2) = 0$, $\det \mathbf{M}_{\mathcal{A}}(\omega^2) = 0$, a numerical procedure was used. The essential steps of the algorithm can be summarized as follows.

To fix the ideas, the case of x_1-symmetric eigenfunctions will be considered. Let the x_1-wave number β_n be given, e.g. $\beta_n = (n\pi/a)^2$, $n = 1, 2, \ldots$. Once a value for ω was set, say $\widetilde{\omega}$, fourth order polynomial equation (4.12) in the

variable $q = \sqrt{z}$, was solved and the expression of the general solution to ordinary differential equation (4.8) was determined. Next, by imposing the boundary conditions, the value of $\det \mathbf{M}_{\mathcal{S}}(\widetilde{\omega}^2)$ was calculated. By repeating this procedure for $\widetilde{\omega} + \Delta\omega$, where $\Delta\omega$ is a proper increment, a graph of $\det \mathbf{M}_{\mathcal{S}}(\omega^2)$ was reconstructed in the given frequency interval. Eigenfrequency values were evaluated by a bisection method applied between two consecutive values of the ω variable corresponding to the change of sign of $\det \mathbf{M}_{\mathcal{S}}(\omega^2)$. For each eigenfrequency value, after solving $\mathbf{M}_{\mathcal{S}}\boldsymbol{c}_{\mathcal{S}} = \mathbf{0}$, the vector $\boldsymbol{c}_{\mathcal{S}}$ of the constants of integration was calculated and, therefore, the corresponding mode of vibration was determined.

5. Application to Zigana bridge

The analysis presented in the preceding Section was applied to determine a class of eigenpairs of Zigana Bridge, namely the vibrating modes antisymmetrical about the x_2-axis in Fig. 3.

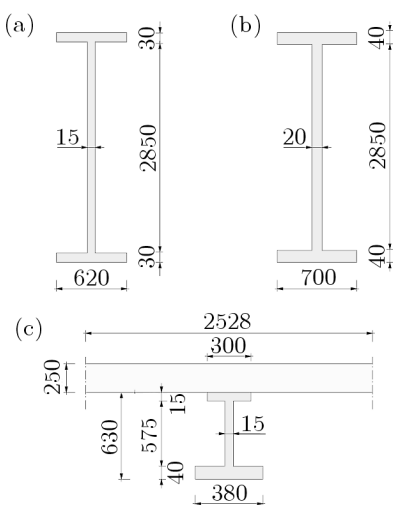

Fig. 4. Dimensional details of Zigana bridge: (a) longitudinal lateral double-T steel beams, (b) longitudinal central double-T steel beam, (c) transverse double-T steel beam (lengths in millimeters)

In Table 1, the geometrical, inertial and mechanical parameters of the bridge are presented. In particular, by neglecting the effect of transverse contraction, see (Timoshenko, 1959), the rigidities of the deck are calculated by means of the expressions

$$D_{11} = \frac{E_c h^3}{12(1-\nu_c^2)} \qquad D_{22} = \frac{E_s I_s^{(hom)}}{a_1}$$
$$D_{12} = \frac{G_c h^3}{12} + \frac{C}{2a_1} \tag{5.1}$$

Table 1. Geometrical, inertial and mechanical parameters of Zigana bridge

Parameter	Symbol	Value
Span length	a	31 m
Deck width	b	13 m
Plate thickness	h	0.25 m
Spacing between stiffeners	a_1	2.528 m
Young's modulus of steel	E_s	$2.1 \cdot 10^{11}\,\mathrm{Nm}^{-2}$
Young's modulus of concrete	E_c	$3.0605 \cdot 10^{10}\,\mathrm{Nm}^{-2}$
Homogenization factor steel-concrete	$n = E_s/E_c$	5.833
Poisson's ratio for steel	ν_s	0.3
Poisson's ratio for concrete	ν_c	0.2
Mass density of steel	ρ_s	$7850\,\mathrm{kgm}^{-3}$
Mass density of concrete	ρ_c	$2450\,\mathrm{kgm}^{-3}$
Plate bending stiffness (x_2-axis)	D_{11}	$4.89 \cdot 10^7$ Nm
Plate bending stiffness (x_1-axis)	D_{22}	$7.41 \cdot 10^8$ Nm
Plate torsional stiffness	D_{12}	$1.97 \cdot 10^7$ Nm

In the foregoing formulas, E_c, E_s are Young's moduli of concrete and steel, respectively; G_c is the shear modulus of concrete; ν_c is Poisson's coefficient of concrete; h is the plate thickness; a_1 is the spacing of the steel transversal beams in the x_1 direction. In Eq. (5.1), $I_s^{(hom)}$ is the moment of inertia, for unit length, of the section formed by the r.c. slab and one stiffener evaluated for the whole section homogenized to steel (with homogenization factor $n = E_s/E_c$), see Fig. 4. The quantity C is the torsional rigidity of a single transversal steel beam and it has been evaluated accordingly to classical theories for thin walled beams with open cross sections, see, for example, (Timoshenko, 1959).

In Table 2, for every value of n, $n = 1, \ldots, 5$, the natural frequencies of the first four free x_1-symmetric and x_1-antisymmetric vibration modes of the bridge are collected. As an example, the shape of vibrating modes corresponding to the lower six natural frequencies are presented in Fig. 5 for the whole bridge deck. Generally speaking, lowest vibration modes are influenced by deformation of the longitudinal plate girders. In the first mode $w^S_{1,1}$, at $f = 3.23$ Hz, the deformed shape of all the three longitudinal beams is similar

Table 2. Theoretical values of natural frequencies of x_1-symmetric modes $w^{\mathcal{S}}_{n,m}$ and of x_1-antisymmetric modes $w^{\mathcal{A}}_{n,m}$ of Zigana bridge, for $n, m = 1, \ldots, 4$

n	m	Frequency $w^{\mathcal{S}}_{n,m}$ [Hz]	Frequency $w^{\mathcal{A}}_{n,m}$ [Hz]
1	1	3.23	4.13
	2	5.40	14.89
	3	19.86	46.96
	4	54.11	99.07
2	1	8.77	9.70
	2	19.79	24.78
	3	30.35	49.54
	4	57.59	100.04
3	1	11.26	11.53
	2	34.25	37.81
	3	55.09	65.03
	4	74.62	104.55
4	1	13.56	13.65
	2	40.36	41.71
	3	78.52	85.50
	4	109.76	125.28

to the first bending mode of the continuous two-span beam. The second mode $w^{\mathcal{A}}_{1,1}$, at $f = 4.13\,\text{Hz}$, has torsional character since the vertical deflection of the central girder is negligible and the two lateral beams vibrate out-of-phase following the fundamental mode of the simply supported two-span continuous beam. In the third mode $w^{\mathcal{S}}_{1,2}$, at $f = 5.40\,\text{Hz}$, the two lateral girders vibrate in-phase according to the fundamental mode of the simply supported two-span beam, whereas the central girder has a similar shape but opposite phase. Higher modes have more pronounced wavy character.

Table 3. Comparison between experimental and theoretical values of the first natural frequencies. Error $= 100 \cdot (f^{theor} - f^{exp})/f^{exp}$

Experimental mode order	Experimental value [Hz]	Theoretical mode order	Theoretical value [Hz]	Error
1	3.13	$w^{\mathcal{S}}_{1,1}$	3.23	3.19
2	4.00	$w^{\mathcal{A}}_{1,1}$	4.13	3.25
5	6.04	$w^{\mathcal{S}}_{1,2}$	5.40	−10.60

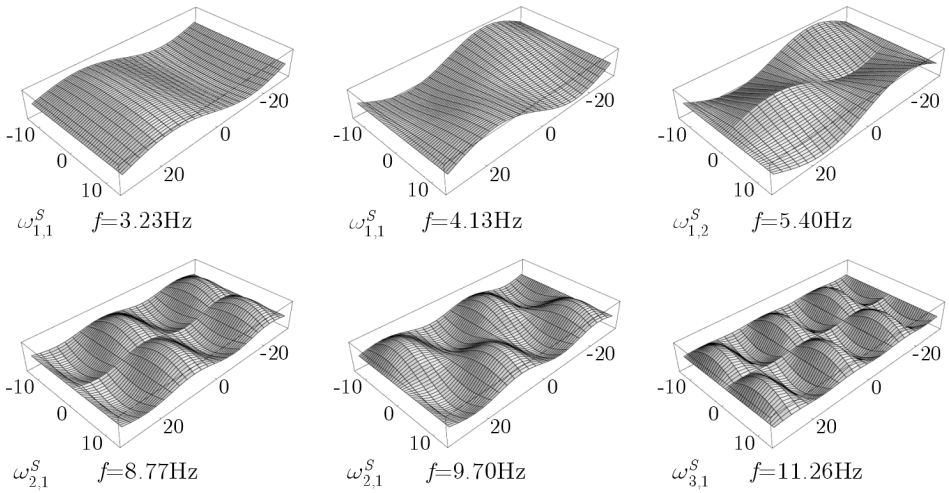

Fig. 5. 3D view of the first six theoretical x_2-antisymmetrical mode shapes of Zigana bridge

Finally, Table 3 compares the computed and experimental frequencies of the lower modes of the bridge. The latter were extracted from frequency response measurements carried out on Zigana bridge by means of a stepped-sine technique, see (Morassi and Tonon, 2008b) for more details on dynamic testing. In brief, the bridge was excited with an electro-mechanical actuator mounted in the vertical direction on the bridge deck, at one fourth of the mid span of the lateral side, see Fig. 6. The transversal motions of the deck were measured by using twelve accelerometers and four seismometers. Based on this experimental set-up, the frequency response functions (FRFs) of the bridge deck were simultaneously determined within the frequency range 0-15 Hz with resolution 0.1 Hz in 1.0-2.5 Hz, 0.02 Hz in 2.5-9.0 Hz and 0.04 Hz for frequencies greater than 9.0 Hz. Each FRF term was computed according to the stepped-sine technique, and formally it was obtained as the ratio between the discrete Fourier transform (DFT) of the accelerometer output signal and the DFT of the force input signal. Figure 7 shows an example of measurements.

Modal components and natural frequencies were extracted from the measured FRFs evaluated between the excitation point and the response points by means of a multiple curve-fitting modal analysis technique, see Ewins (2000). The curve fitting procedure assumes a FRF term given as the ratio between the numerator polynomial and the denominator polynomial of a suitable order. A numerical algorithm based on an iterative least-squared method was used to obtain the optimal values of the modal parameters, see, as an example,

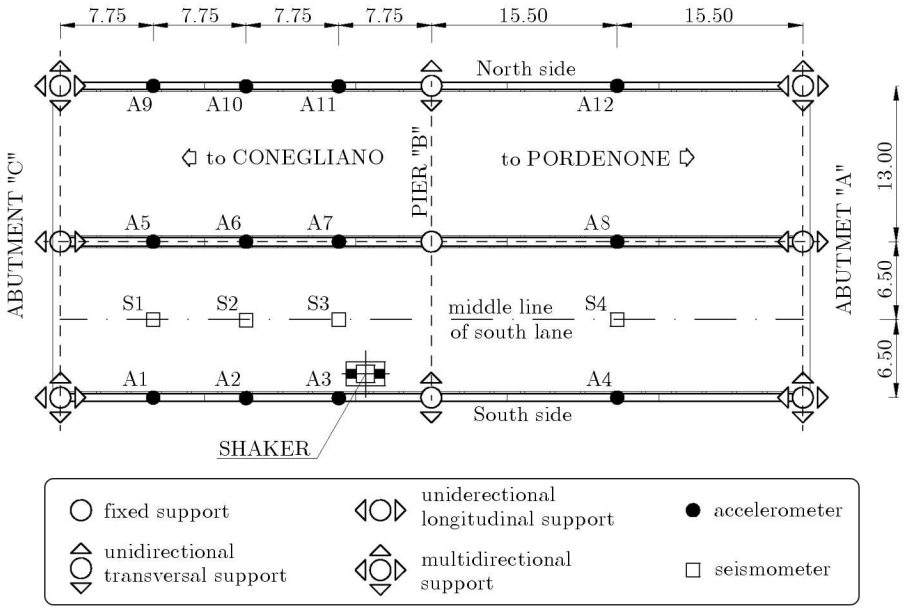

Fig. 6. Instrumental layout and bridge supports

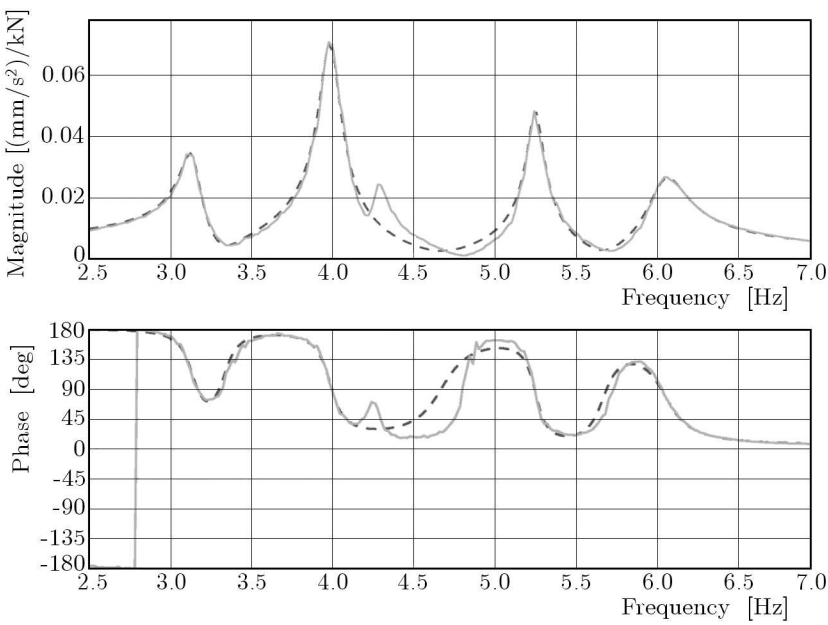

Fig. 7. Zigana bridge: example of comparison between measured (continuous line) and synthesized (dashed line) point inertance

Fig. 7. More precisely, five, three and five vibrating modes were identified in the frequency intervals 2.5-7 Hz, 7-9 Hz and 9-15 Hz, respectively.

The experimental mode shapes in Fig. 8 correspond to linear interpolation of the measured modal components. Visual comparison and Modal Assurance Criterion allow one to confirm the correspondence between the first (3.13 Hz), second (4.00 Hz) and fifth (6.04 Hz) experimental modes and the theoretical modes $w^{\mathcal{S}}_{1,1}$, $w^{\mathcal{A}}_{1,1}$, $w^{\mathcal{S}}_{1,2}$, respectively, as it is shown in Table 3. The results of Table 3 show that the percentage differences between the experimental and theoretical natural frequency values are rather small, even when compared with the refined finite element model of the whole bridge developed by Morassi and Tonon (2008b). Therefore, the analytical model of the bridge can be considered satisfactory for practical engineering applications.

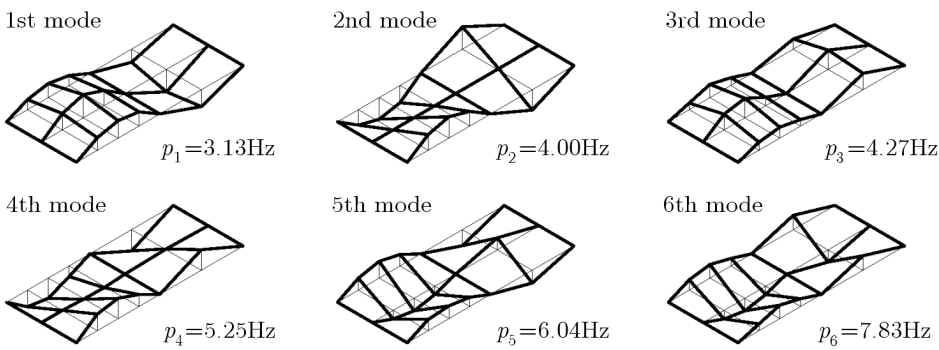

Fig. 8. 3D view of the first six experimental mode shapes of Zigana bridge

6. Concluding remarks

In this paper, a class of free vibrations of a two-span, two-lane steel-concrete bridge has been studied. The eigenvalue problem concerns with vibration of two thin, homogeneous, orthotropic, rectangular plates connected by cylindrical hinges to a reinforcing beam running along the common edge. Each plate is stiffened along the external edge parallel to the common edge and simply supported along the other two orthogonal edges. This combination of boundary and jump conditions seems not to be considered in the literature before. The classical method of separation of variables has been used to find a class of exact eigenpairs of the system. Analytical values of the first lower natural frequencies agree well with those obtained in dynamic tests carried out on the

real bridge. The analytical model of the bridge will be of valuable importance in the design of new bridges of the same class and on its use as the reference model for future structural identification analyzes.

Acknowledgements

The authors wish to thank Dr. Michele Dilena for useful suggestions on the numerical algorithm used to find the roots of the characteristic equation.

References

1. Aktan A.E., Farhey D.N., Helmicki A.J., Brown D.L., Hunt V.J., Lee K.-L., Levi A., 1997, Structural identification for condition assessment: experimental arts, *Journal of Structural Engineering ASCE*, **123**, 12, 1674-1684
2. Brezis H., 1986, *Analisi funzionale*, Liguore Editore, Napoli
3. Catbas F.N., Ciloglu S.K., Hasancebi O., Grimmelsman K., Aktan A.E., 2007, Limitations in structural identification of large constructed structures, *Journal of Structural Engineering ASCE*, **133**, 8, 1051-1066
4. Cox H.L., Benfield W.A., 1959, Vibration of uniform square plates bounded by flexible beams, *Journal of the Acoustic Society of America*, **31**, 7, 963-966
5. Dilena M., Morassi A., 2011, Dynamic testing of a damaged bridge, *Mechanical Systems and Signal Processing*, **25**, 5, 1485-1507
6. Elishakoff I., Sternberg A., 1980, Vibration of rectangular plates with edge-beams, *Acta Mechanica*, **36**, 195-212
7. Ewins D.J., 2000, *Modal Testing: Theory, Practice and Application*, Research Studies Press Ltd, Baldock, Hertfordshire
8. Gentile C., 2006, Modal and structural identification of a RC arch bridge, *Structural Engineering and Mechanics*, **22**, 1, 53-70
9. Gentile C., Cabrera F.M., 1997, Dynamic investigation of a repaired cable-stayed bridge, *Earthquake Engineering and Structural Dynamics*, **26**, 1, 41-59
10. Gorman D.J., 2003, Free vibration analysis of corner-supported rectangular plates with symmetrically distributed edge beams, *Journal of Sound and Vibration*, **263**, 979-1003
11. Gorman D.J., Garibaldi L., 2006, Accurate analytical type solutions for free vibration frequencies and mode shapes of multi-span bridge decks: the span-by-span approach, *Journal of Sound and Vibration*, **290**, 321-336
12. Jaishi B., Ren W.X., 2005, Structural finite element model updating using vibration test results, *Journal of Structural Engineering ASCE*, **131**, 4, 617-628

13. Leissa A.W., 1973, The free vibration of rectangular plates, *Journal of Sound and Vibration*, **31**, 3, 257-293

14. Li Q.S., 2000, Exact solutions for free vibration of multi-step orthotropic shear plates, *Structural Engineering and Mechanics*, **9**, 3, 269-288

15. Marcuzzi A., Morassi A., 2010, Dynamic identification of a concrete bridge with orthotropic plate-type deck, *Journal of Structural Engineering ASCE*, **136**, 5, 586-602

16. Morassi A., Tonon S., 2008a, Dynamic testing for structural identification of a bridge, *Journal of Bridge Engineering ASCE*, **13**, 6, 573-585

17. Morassi A., Tonon S., 2008b, Experimental and analytical study of a steel-concrete bridge, *Journal of Vibration and Control*, **14**, 6, 771-794

18. Morassi A., Vestroni F. (Eds.), 2008, *Dynamic Methods for Damage Identification in Structures*, CISM Courses and Lectures No. 499, Springer, Wien

19. Timoshenko S.P., Woinowsky-Krieger S., 1959, *Theory of Plates and Shells*, McGraw-Hill, New York

20. Voigt W., 1893, Bemerkung zu dem Problem der transversalen Schwingungen rechteckiger Platten, *Nach. Ges. Wiss.* (Göttingen), **6**, 225-230

21. Weinberger H.F., 1965, *A First Course in Partial Differential Equations*, Dover Publications Inc., New York

Dokładne rozwiązania zagadnienia drgań swobodnych konstrukcji mostu stalowo-betonowego

Streszczenie

Praca dotyczy analizy pewnej klasy drgań swobodnych dwuprzęsłowego, dwujezdniowego mostu stalowo-betonowego. Przęsło zamodelowano jako cienką, jednorodną, ortotropową płytę usztywnioną belkami zamocowanymi w kierunku wzdłużnym mostu. Do znalezienia dokładnych rozwiązań problemu drgań swobodnych modelu zastosowano metodę rozdzielenia zmiennych. Na koniec zaprezentowano i przedyskutowano porównanie częstości własnych i postaci drgań własnych modelu z wynikami zarejestrowanymi na rzeczywistej konstrukcji.

Manuscript received March 14, 2011; accepted for print May 13, 2011